JOC The Journal of Organic Chemistry

Article

pubs.acs.org/joc

Fluorescent Modular Boron Systems Based on NNN- and ONO-Tridentate Ligands: Self-Assembly and Cell Imaging

Christoph Glotzbach,[†] Ulrike Kauscher,[†] Jens Voskuhl,[†] N. Seda Kehr,[‡] Marc C. A. Stuart,[#] Roland Fröhlich,[†] Hans J. Galla,[§] Bart Jan Ravoo,[†] Kazuhiko Nagura,[∥] Shohei Saito,[∥] Shigehiro Yamaguchi,*[,∥] and Ernst-Ulrich Würthwein*[,†]

[†]Organic Chemistry Institute, Westfälische Wilhelms-Universität, Corrensstr. 40, 48149 Münster, Germany

[‡]Physical Institute, Westfälische Wilhelms-Universität, Heisenbergstrasse 11, 48149 Münster, Germany

[#]Biophysical Chemistry, Biomolecular Sciences and Biotechnology Institute, 9747 AG Groningen, The Netherlands

[§]Biochemistry Institute, Westfälische Wilhelms-Universität, Wilhelm-Klemm-Str. 2, 48149 Münster, Germany

[∥]Department of Chemistry, Graduate School of Science, Nagoya University, Furo, Chikusa, Nagoya 464-8602, Japan

Supporting Information

ABSTRACT: We have synthesized a series of new fluorescent boron systems **1a−c** and **2a−d** based on nitrogen (NNN) or nitrogen and oxygen (ONO)-containing tridentate ligands. These novel dyes are characterized by high thermal and chemical stability. They show large Stokes shifts (mostly above 3200 cm^{-1}) and quantum yields in solution and in the solid state up to 40%. The easy, modular synthesis facilitates the convenient variation of the axial substituent on the central boron atom, allowing the functionalization of this dye for biochemical use. Introducing a long alkyl chain with a phenyl spacer at this axial position enables the self-assembly of the boron compound **2d** to form a fluorescent vesicle, which is able to encapsulate small molecules such as sulforhodamine. Additionally, boron compound **2d** was found to serve as a dye for cell imaging since it has the capability of binding to the nuclear membranes of HeLa cells. With phospholipids such as DOPC, giant unilamelar vesicles (GUV) are formed. These results demonstrate the wide applicability of this new boron system in supramolecular and medicinal chemistry.

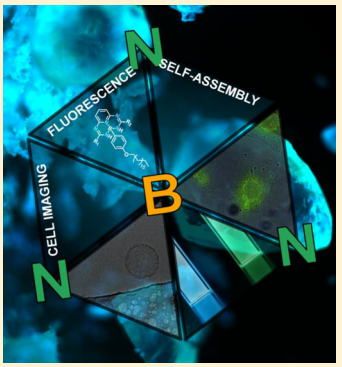

INTRODUCTION

Fluorescent organoboron compounds have been extensively studied.[1] Their photophysical properties are being utilized in many fields of current research, such as biochemical probes,[2] organic light-emitting diodes,[3] and other advanced materials.[4] Despite the fact that there is a sheer unlimited number of dyes available for research, there is still considerable interest in new dyes that are easily accessible and show unique properties.[5] Among organoboron compounds, boron complexes based on tridentate ligands possess a unique position due to their facile functionalization at the axial position on the central boron atom.[6]

In this work, we develop the novel boron system **II** by extending the previously reported bidentate ligand (1,3,5-triazapenta-1,3-diene) **I**[7] to tridentate ligands (Scheme 1). By introducing a pyridine substructure to connect R^1 and R^2 and a subsequent addition of a second arm at the ortho position of the pyridine ring, more π-extended boron complexes are formed, which may lead to an improvement of the fluorescence properties. These compounds, whose quantum yields are up to 40% in solution and in the solid state, show high thermal and chemical stability, which are preconditions for a broad range of applications. The emission wavelength can be tuned by facile structural modifications on the coordinating atoms (ONO or NNN combinations) and the terminal substituents of the π-conjugated ligand.

Scheme 1. Enhancement of Previously Reported Boron Compound I[7] to Boron Complexes II Based on Tridentate Ligands

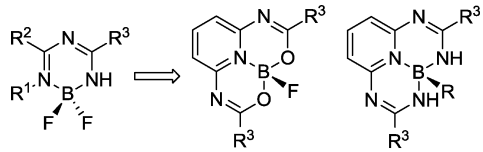

I II

We also employ one of the emissive boron complexes as a building block for vesicles, which shows the ability to encapsulate small molecules in aqueous media. Furthermore, cell-imaging experiments demonstrate the utility of our new dye system in biochemical and medicinal research fields.

RESULTS AND DISCUSSION

Synthesis. A significant advantage of the system presented herein is its modular and large-scale synthesis from readily

Received: February 25, 2013
Published: April 15, 2013

   dx.doi.org/10.1021/jo4003745 | J. Org. Chem. 2013, 78, 4410−4418

available building blocks such as amines, acyl chlorides, nitriles, and boronic acids (Scheme 2). Both, the ONO- (**3a–c**) and the NNN-tridentate ligands (**4a–c**) are built up from 2,6-diaminopyridine as a central building block.

Scheme 2. Synthesis of Boron Complexes Based on (A) ONO- and (B) NNN-Tridentate Ligands

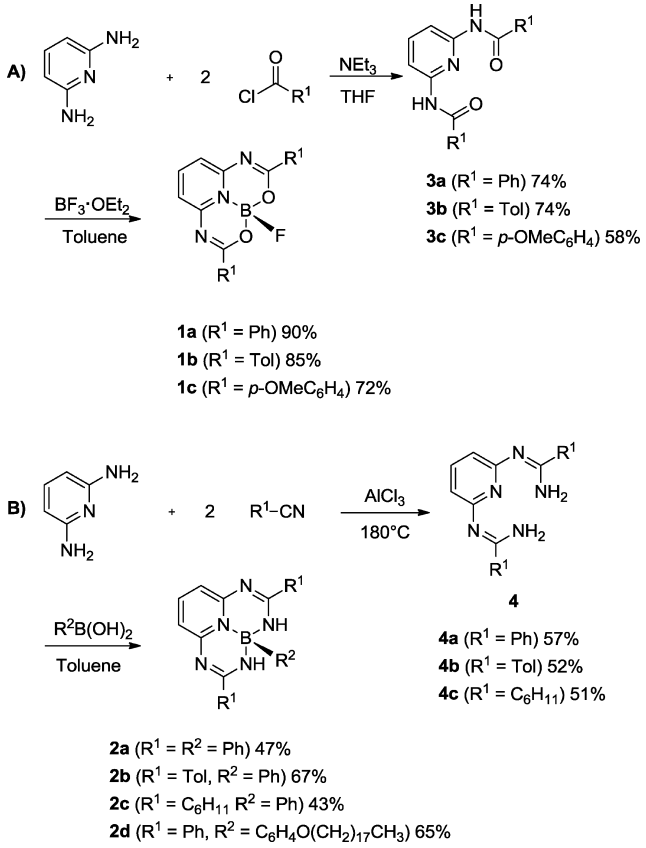

For the preparation of the ONO-tridentate ligands **3a–c**, 2,6-diaminopyridine was treated with 2 equiv of the respective acyl chlorides.[8] The resulting bis-amides were treated with an excess amount of $BF_3{\cdot}OEt_2$ in the presence of triethylamine to tailor the novel luminescent boron complexes **1a–c** in 72–90% yield. The NNN-tridentate ligands **4a–c**, which serve as precursors for **2a–d**, were synthesized by a simple reaction of the corresponding nitriles with 2,6-diaminopyridine in the presence of $AlCl_3$. This procedure, previously reported for aromatic bis-amidines,[9] could also be applied to obtain the aliphatic bis-amidine **4c** employed for the synthesis of compound **2c**.

The key step is the introduction of the boron moiety including the R^2 substituent, which enables versatile functionalization of this system (see below). The emissive boron complexes **2a–d** were obtained from the ligands **4a–c** either by treatment with boronic acids $R^2B(OH)_2$ or by using triaryl boranes BR^2_3. Refluxing a solution of **4a–c** and the corresponding boronic acid (or triarylborane) in toluene gave **2a–d** in 43–67% yield. The simple structural modification by introducing the axial R^2 group using small building blocks facilitates an easy tuning of the system to match the users' interest, which is exemplarily shown by introducing a long alkyl chain at the R^2 substituent (**2d**). The corresponding boronic acid with the C_{18} alkyl chain was readily prepared by a literature procedure.[10]

Photophysical Properties in Solution. The boron complexes obtained from the ONO-tridentate ligands (**1a,b**) exhibit blue emissions at λ_{em} = 456–457 nm (Figure 1A, Table 1), while their longest wavelength absorption bands are observed at λ_{abs} = 394 nm. Introduction of the electron-donating OMe substituent at the terminal R^1 aryl groups (**1c**) leads to only a small bathochromic shift of the absorption (λ_{abs} = 399 nm) and fluorescence maxima (λ_{em} = 460 nm), while the molar extinction coefficient is significantly increased from ε_{max} = 28 000 M^{-1} cm^{-1} for **1a** to ε_{max} = 71 500 M^{-1} cm^{-1} for **1c**.

The luminescence quantum yield was increased from **1a** (R^1 = Ph, Φ_F = 0.20) over **1b** (R^1 = Tol, Φ_F = 0.30) to **1c** (R^1 = *p*-$OMeC_6H_4$, Φ_F = 0.39). Short lifetimes of the emission with τ_F = 1.3–1.8 ns confirm that the observed luminescence corresponds to a radiative decay process from a singlet excited state, namely, fluorescence, rather than phosphorescence. On the basis of the quantum yields and lifetimes, the rate constants of radiative and nonradiative decay from the singlet excited state for **1a–c** are estimated to be k_r = 1.5–2.2 × 10^8 s^{-1} and k_{nr} = 3.5–6.1 × 10^8 s^{-1}, respectively.

Going from the ONO-tridentate compounds (**1a,b**) to the more electron-rich NNN-systems (**2a,b**), results in a significant bathochromic shift in both the absorption (λ_{abs} = 435–440 nm) and fluorescence maximum wavelengths (λ_{em} = 508–513 nm) (Figure 1B, Table 1). A bright green emission is observed in solution, although the quantum yields are relatively low with values between Φ_F = 0.13 and Φ_F = 0.21. The analysis of the decay rate constants for **2a** (k_r = 5.2 × 10^7 s^{-1}) and **2b** (k_r = 8.1 × 10^7 s^{-1}) suggests that the smaller k_r values are responsible for the lower quantum yields since the nonradiative decay rate constants k_{nr} = 3.5 × 10^8 s^{-1} for **2a** and k_{nr} = 3.1 × 10^8 s^{-1} for **2b** are not significantly different from those of **1a** (k_{nr} = 6.1 × 10^8 s^{-1}) and **1b** (k_{nr} = 4.5 × 10^8 s^{-1}).

The replacement of the terminal aryl substituents at the R^1 position by an aliphatic group (**2c**) leads to a significant

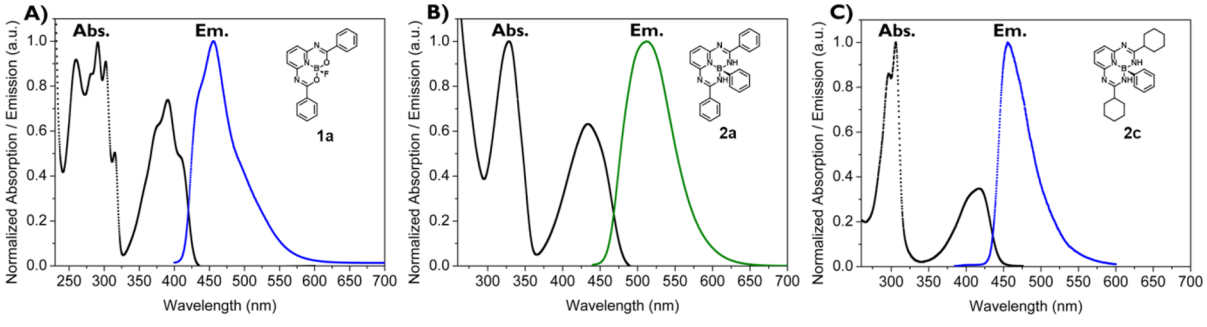

Figure 1. Normalized absorption and emission spectra of (A) compound **1a**, (B) compound **2a**, and (C) compound **2c**.

dx.doi.org/10.1021/jo4003745 | J. Org. Chem. 2013, 78, 4410–4418

Table 1. Photophysical Data of the Boron Complexes

compound	λ_{abs} [a] (nm)	λ_{em} [b] (nm)	$\Delta\nu$ [c] (cm^{-1})	ε_{max} [d] (M^{-1} cm^{-1})	Φ_F [e]	τ_F [f] (ns)	k_r [g] (s^{-1})	k_{nr} [h] (s^{-1})
1a	394	456	3500	28 000	0.20/0.38	1.3	1.5×10^8	6.1×10^8
1b	394	457	3500	43 200	0.30/0.40	1.6	1.9×10^8	4.5×10^8
1c	399	460	3300	71 500	0.39/0.41	1.8	2.2×10^8	3.5×10^8
2a	440	513	3200	17 500	0.13/0.15	2.5	5.2×10^7	3.5×10^8
2b	435	508	3300	18 700	0.21/0.20	2.6	8.1×10^7	3.1×10^8
2c	416	456	2100	22 200	0.10/0.14	4.6	2.2×10^7	2.0×10^8
2d	431	511	3600	21 000	0.14/0.14	2.2	6.3×10^7	3.8×10^8

[a]Longest wavelength absorption maximum recorded in dichloromethane. [b]Fluorescence maximum. [c]Stokes shift in cm^{-1} as calculated from the λ_{abs} and λ_{em} data. [d]Molar extinction coefficient at the longest-wavelength absorption maximum. [e]Absolute fluorescence quantum yield determined by a calibrated integration sphere system. Quantum yields are given for solution/solid state. [f]Fluorescence lifetimes were measured in solution using a pulsed picosecond laser (377 nm) and were fit to single exponential decays with $R^2 > 0.99$. [g]Rate constant of radiative decay calculated using the equation $k_r = \Phi_F/\tau_F$. [h]Rate constant of nonradiative decay calculated using the equation $k_{nr} = (\Phi_F - 1)/\tau_F$.

hypsochromic shift in fluorescence (λ_{em} = 456 nm) (Figure 1C, Table 1), which is attributed to its shorter π-conjugation in comparison to the aromatic substituted boron complex **2a**. In other words, the aryl substituents R^1 are an important factor for the green emission of **2a**, **2b**, and **2d**. The possibility of excimer formation was ruled out, since there was no concentration dependence in the shape of fluorescence spectra for either the ONO- or the NNN-system (Supporting Information).

The large Stokes shifts (Table 1) of compounds **1** and **2** (except **2c**) are interesting photophysical features, especially for applications. Calculated on the basis of the maxima of the relatively broad and structured absorption and emission bands (see Figure 1 and Supporting Information), they amount to around 3200−3600 cm^{-1} and result in an only small spectral overlap between absorption and fluorescence. This is clearly an advantage of these boron complexes as a fluorescent dye in comparison to typical BODIPY derivatives, having small Stokes shifts of 400−1000 cm^{-1}.[1e] Generally, a larger Stokes shift is beneficial to suppress the reabsorption of the fluorescence in the condensed phase, which leads to emission quenching.

Solvent polarity has only a negligible influence on the fluorescence properties of these boron complexes. The emission spectra of **1a** and **2a** as model compounds were recorded in various solvents with different polarity (Figure S15, Supporting Information). While compound **1a** shows emissions at λ_{em} = 453 nm in methanol and at λ_{em} = 456 nm in toluene, compound **2a** exhibits the emission maxima at λ_{em} = 508 nm in diethylether and DMSO and at λ_{em} = 514 nm in ethyl acetate and toluene. The lack of significant solvatochromism indicates a negligible intramolecular charge transfer (ICT) character of these systems.

Solid-State Emission and Crystal Structures. Interestingly, these complexes show an intense blue and green emission even in the solid state (Table 1, Figure 2, Figure S14 in Supporting Information). In general, fluorescence quenching often takes place in the solid state due to close packing, resulting in energy transfer and reabsorption of fluorescence.[11] The quantum yields of **1** in the crystalline state are comparably high (Φ_F = 0.38−0.41) among other reported boron complexes based on tridentate ligands.[6] Although the Φ_F values in the solid state of **2** are relatively low with Φ_F = 0.14−0.20, the bright green luminescence in the solid state (and also in solution) enables its biochemical use as demonstrated by compound **2d** in cell imaging experiments (*vide infra*).

To gain insight into the solid-state structures, single crystal X-ray diffraction analyses were conducted for **1a**, **1c**, **2b**, and **2c** (Figure 2 and Supporting Information). In both series of

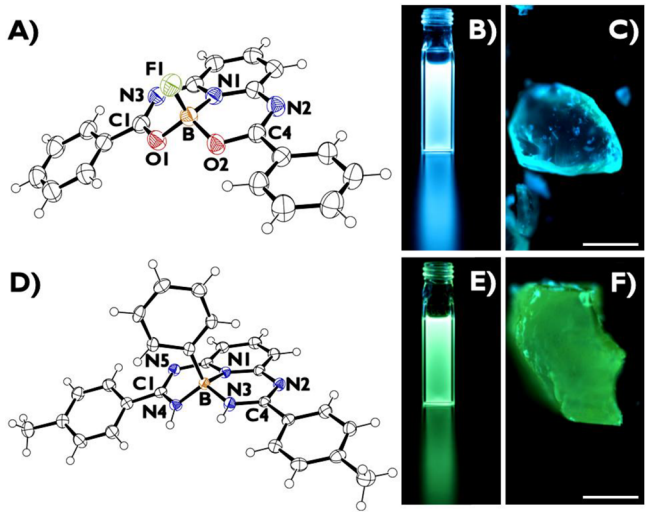

Figure 2. (A) ORTEP plot (thermal ellipsoids with 50% probability) of the molecular structure of **1a**. Selected bond lengths (Å) and dihedral angles (deg) for **1a**: N1−B 1.541(2), O1−B 1.453(2), O2−B 1.449(2), F1−B 1.384(2), N1−B−O2−C4 37.87, and N1−B−O1−C1 33.00. (B) Image of compound **1a** in solution and (C) in the solid state. (D) ORTEP plot (thermal ellipsoids with 50% probability) of the molecular structure of **2b**. Selected bond lengths (Å) and dihedral angles (deg) for **2b**: N1−B 1.556(3), N4−B 1.523(3), N3−B 1.515(3), N1−B−N3−C4 19.25, and N1−B−N4−C1 46.17. (E) Image of compound **2b** in solution and (F) in the solid state. Irradiation was performed with an UV lamp with a wavelength of 366 nm. The scale bar represents 100 μm.

compounds **1** and **2**, the central B atom has a tetrahedral geometry. The sum of two N−B−O angles and O−B−O angle in **1a** is 326.3°, while the sum of three N−B−N angles in **2b** is 324.3° (Figure 2A and D). In both of the structures of **1a** and **2b**, the R^1 aryl groups assume nearly coplanar arrangements to the tricyclic core skeleton, suggesting effective extension of π conjugation. The dihedral angles between the terminal phenyl ring and the C1−O1−N3 or C4−O2−N2 mean planes in **1a** are less than 10°, whereas those between the terminal tolyl groups and the C1−N4−N5 or the C4−N3−N2 mean planes in **2b** are less than 15°.

However, as a result of its almost perpendicular orientation, substituent R^2 does not play a substantial role for the electron delocalization in the phenalene-like heterocyclic plane. This is supported by the very small influence on the emission wavelengths e.g. **2a** versus **2d** (Table 1). As all crystal structures show, the molecules are packed in a staggered way

dx.doi.org/10.1021/jo4003745 | J. Org. Chem. 2013, 78, 4410−4418

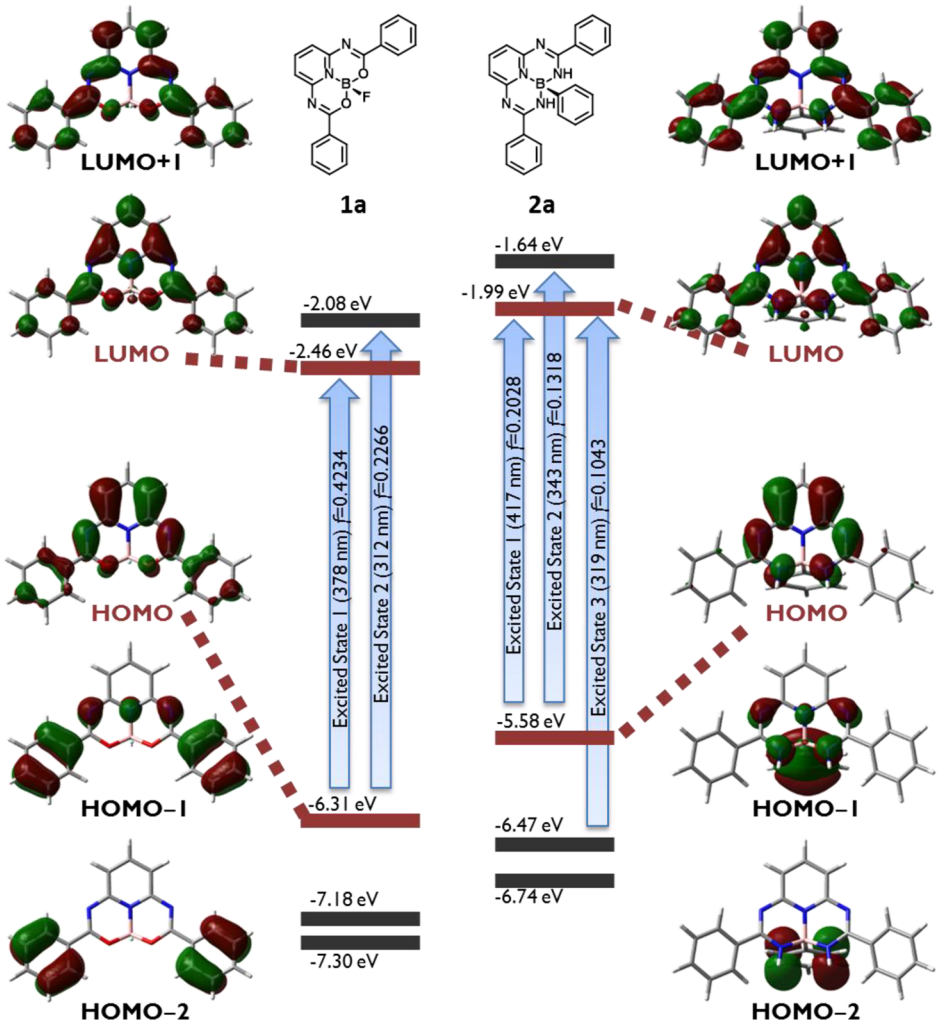

Figure 3. Kohn–Sham molecular orbitals of **1a** and **2b** as representative compounds for the ONO- and NNN-systems.

with marginal overlap of the π-systems. The perpendicular orientation of the axial R^2 substituents to the π-conjugated tricyclic plane prevents the chromophores from stacking closely. Thus, there seem to be no significant interactions such as π-stacking or other possible short contact interactions. This should be partly responsible for their high quantum yields in the crystalline state. For example, compound **2a** shows an identical emission at λ_{em} = 513 nm in solution (e.g., in dichloromethane) and in the solid state, since the phenyl group at the R^2 position keeps the chromophores separate. The emission maximum of **1a** at λ_{em} = 456 nm in solution is slightly red-shifted to λ_{em} = 471 nm in the solid state. This may be due to the fact that the fluorine atom at the R^2 position is relatively small and a closer packing is possible.

Quantum Chemical Calculations. To investigate the electronic structures and the electronic transitions of these π-conjugated boron complexes, DFT geometry optimizations followed by TD-DFT calculations at the B3LYP[12]/def2-TZVP level were carried out for all compounds (see Supporting Information). The Kohn–Sham molecular orbitals of **1a** and **2a** as model compounds for the ONO- and NNN-tridentate systems are shown in Figure 3.

The TD-DFT calculations reproduce the bathochromic shifts of the absorption maxima from the ONO-ligand-coordinated boron complexes **1a–c** to the NNN-ligand-coordinated **2a–d** (Supporting Information). These shifts are due to the energy difference in their HOMO–LUMO gaps. While the HOMO–LUMO gap for **1a** is 3.85 eV, **2a** has a smaller gap of 3.59 eV (Figure 3). This difference is mainly attributed to the more significant difference in the HOMO level compared to that in the LUMO level. The much higher-lying HOMO in **2a** compared to **1a** is regarded to be the origin of the bathochromic shift due to the more pronounced electron-donating character of the N atoms compared to the O atoms (Figure S3, Supporting Information).

To visualize the contributions of the molecular moieties to the HOMO and LUMO and the different transitions upon irradiation (UV–vis spectra), TD-DFT calculations for 20 states of compound **2a** were calculated for the gas phase using the B3LYP[12] functional and the def2-TZVP basis set (Figure S1, Supporting Information). The first excited state (2.97 eV, 417 nm) with a CI coefficient of 0.7 and oscillator strength of 0.2 can clearly be assigned to the HOMO→LUMO transition. The frontier orbital pictures (Figure S2, Supporting Information) show that substituent R^2 is out of the phenalene-like plane of the molecule and contributes to neither the HOMO nor the LUMO of the first excited state; thus, an influence on the emission can be ruled out. This is consistent with our previous claim that, due to the almost perpendicular orientation

dx.doi.org/10.1021/jo4003745 | J. Org. Chem. 2013, 78, 4410–4418

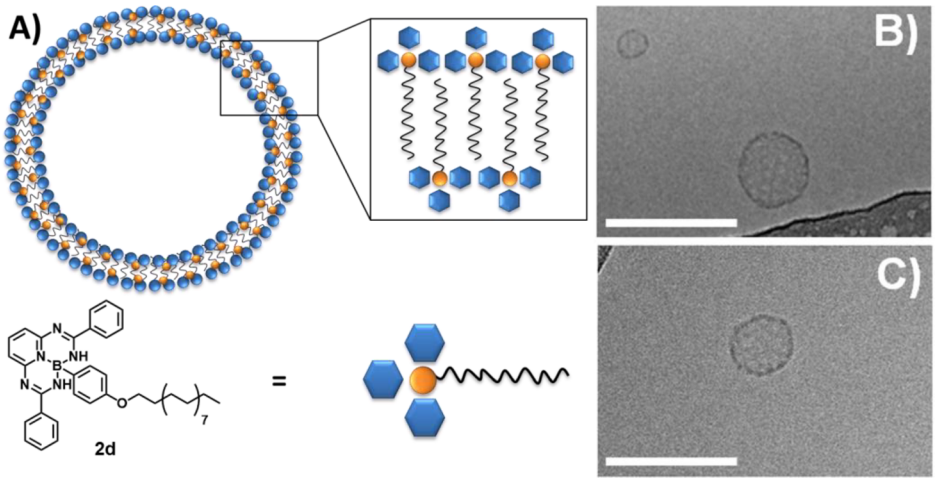

Figure 4. (A) Schematic presentation of the self-assembly of compound **2d** into vesicles. (B, C) Cryo-TEM images of vesicles made from a hydrated film of **2d**, concentrations: [**2d**] = 0.5 mM. For panels B and C the scale bar represents 100 nm.

of R^2, it is unlikely that it plays a substantial role for the electron delocalization in the main π-conjugation.

It should be noted that the terminal R^1 group significantly alters the photophysical properties of these boron complexes. For example, the phenyl-extended **2a** has red-shifted absorption and emission bands by 24 and 57 nm, respectively, compared to the cyclohexyl-substituted **2c**. The DFT calculations reveal that **2a** with its more extended π-conjugation has a lower LUMO level (−1.99 eV) compared to **2c** (−1.55 eV). In contrast, the HOMO levels of **2a** (−5.58 eV) and **2c** (−5.50 eV) are comparable. As a result, the energy for the HOMO−LUMO transition in **2a** becomes smaller (3.59 eV) than that of **2c** (3.94 eV), leading to the observed bathochromic shift (Figure 3 and Figure S4 in Supporting Information).

Studies on the solvatochromic behavior were done by calculating (CAM-B3LYP[13]/def2-TZVP) the dipole moments in the ground state (μ_G) and the first excited state (μ_E) of **1a** and **2a** and comparing them to those of Brookers Dye, a well-known chromophore[14] that shows high sensitivity to solvent polarity. This is a useful approach to theoretically investigate solvatochromic behavior of fluorescent nitrogen−boron compounds.[15] The dipole moments of **1a** and **2a** in the first excited state were calculated to be quite small with values of μ_E = 2.7 D for **1a** and μ_E = 3.9 D for **2a** compared to Brookers Dye with μ_E = 17.6 D. The differences of the dipole moments between the ground state and the first excited state amount to only $\Delta\mu_{E\text{-}G}$ = 0.2 D for **1a** and $\Delta\mu_{E\text{-}G}$ = 0.7 D for **2a**, but to $\Delta\mu_{E\text{-}G}$ = 2.4 D for Brookers Dye. This correlates well with the experimentally observed lack of solvatochromism.

We are also interested in the electronic contribution exerted by the axial R^2 ligand on these boron-centered π-conjugated systems. The R^2 substituent is not relevant to the electron delocalization in the tricyclic system due to its almost perpendicular orientation. The calculation showed that the axial R^2 moiety influences only the HOMO−1 and HOMO−2 in **2a** (Figure 3). As the longest absorption band and the emission band are only related to the electronic transition from HOMO to LUMO, the R^2 group does not affect these photophysical properties. Indeed, compounds **2a** and **2d** have almost identical λ_{abs} and λ_{em} compared to each other (Table 1). This negligible effect of the R^2 substituent on the fluorescence properties suggests the promising use of this moiety as an interconnection of the chromophore to a large variety of application-related functional groups. For example, the fluorescent dye may serve as a lipid anchor for bioactive molecules. From this point of view, we introduced an aliphatic moiety to **2d** and explored its ability of self-assembly into vesicles (*vide infra*).

Self-Assembly. Amphiphilic molecules can self-assemble into complex structures in different media via various kinds of noncovalent interactions such as van der Waals, electrostatic, and hydrophobic interactions as well as hydrogen bonding. In particular, liposomes and vesicles are interesting supramolecular substances with a bilayer membrane structure.[16,17] They have unique properties, such as encapsulation of dyes and drugs and thus have potential as transporters in an aqueous environment. Although vesicles composed of fluorescently labeled lipids and vesicles labeled with hydrophobic dyes are well-known, there are only a few examples of the assembly of vesicles from amphiphilic fluorescent dyes.[18] The self-assembly of fluorescent boron amphiphiles, e.g., boron quinolate block copolymers[19] or BODIPY block copolymers,[20] to form supramolecular structures is also a thriving field of current research.[21]

To investigate the self-assembly properties of compound **2d** in aqueous media, we examined its ability of forming vesicles. Thus, a dried film of **2d** (prepared from 1 mM solution in chloroform) was hydrated with distilled water, sonicated for 3 min, and finally extruded through a polycarbonate membrane with a pore size of 100 nm. DLS measurements of the assemblies revealed the formation of nanostructures of around 100 nm size, which were disrupted by adding the nonionic surfactant Triton X-100 (1 wt %). These results led to the conclusion that vesicular structures are present (Figure S7, Supporting Information). Upon hydration of a film of **2d** in the presence of a sulforhodamine solution at a fluorescence self-quenching concentration (20 mM), it was possible to encapsulate this dye inside the vesicles. Nonencapsulated dye was removed by size exclusion chromatography using Sephadex G50. To check if the sulforhodamine is located in the aqueous compartment of the vesicles, the structures were lysed by adding Triton X-100. The disassembly of the vesicles resulted in a dilution of sulforhodamine, which was detected as a significant increase in fluorescence due to a relief of self-quenching of sulforhodamine (Figure S8, Supporting Information). Finally, Cryo-TEM imaging was performed to further confirm the existence of vesicular structures in aqueous media.

dx.doi.org/10.1021/jo4003745 | J. Org. Chem. 2013, 78, 4410−4418

The Cryo-TEM images indeed showed unilamellar vesicles with an average size of around 80−100 nm. It is obvious that compound **2d** cannot pack as densely as natural phospholipids in a biological membrane (Figure 4). Nevertheless, the encapsulation experiments demonstrate that the vesicles have a semipermeable membrane.

To check whether the amphiphilic compound **2d** can be introduced into membranes of dioleoylphosphatidylcholine (DOPC), the formation of giant unilamelar vesicles (GUV) using the electroformation method was investigated. To this end 20 mol % of compound **2d** was combined with the phospholipid DOPC to prepare a 1 mM solution of amphiphiles in chloroform. Sixteen microliters of the chloroform solution was spread on the electrode slides coated with indium tin oxide (ITO). Then, the chloroform was evaporated in a vacuum oven at 50 °C. The resulting film was hydrated with buffer solution (1 mM HEPES, 100 mM sucrose, pH 7.4). An alternating electric field was applied at 10 Hz and 1 V at 50 °C for 1 h. After this time the species formed were harvested and investigated with a confocal laser scanning microscope. It was found that indeed GUVs were formed showing the characteristic green fluorescence of compound **2d**, proving its successful introduction into the liposomal membrane. To check if microdomains were formed, a z-stack series of images was constructed, and a 3D model was calculated (Figure 5). This

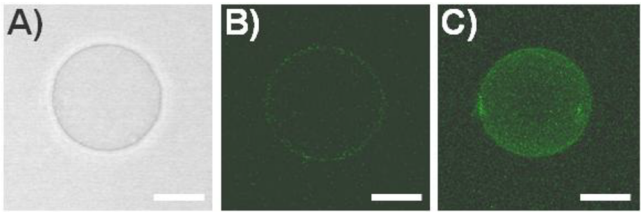

Figure 5. (A) Light microscopy image of a GUV consisting of 80 mol % DOPC and 20 mol % boron compound **2d**. (B) CLSM single image slice through the GUVs equator. (C) z-Stack series of the GUV. The scale bar represents 5 μm.

model shows an even distribution of the fluorescent boron complex on the liposomal surface. With these results in hand, cell imaging studies were conducted to check whether this behavior of compound **2d** is also suitable to label biological membranes in the same fashion.

Cell Imaging. For this purpose, we investigated the ability of compound **2d** to act as a cell marker. Thus, compound **2d** was dissolved in DMSO, and the respective solution was further diluted by adding it to the cell culture media, resulting in a 10^{-3} M solution with less than 1% in DMSO. HeLa cells (derived from cervical cancer) were incubated at 37 °C and 5% CO_2 atmosphere in this media for 4 and 24 h. After the corresponding incubation period, the cells were washed with phosphate buffer solution (PBS), then fixed with 4% paraformaldehyde (PFA) solution, and finally washed again with PBS and water. The fixed cells were analyzed by fluorescence microscopy. The respective microscope images (Figure 6) showed that compound **2d** was internalized after 4 h exclusively into the nuclear membrane. Very similar results were obtained after 24 h of incubation time. In both cases we observed the green emission of **2d**, emerging at the nuclear membrane (Figure S9, Supporting Information).

To investigate effect of **2d** on living cells, its cytotoxicity was determined using a lactate dehydrogenase (LDH) cytotoxicity

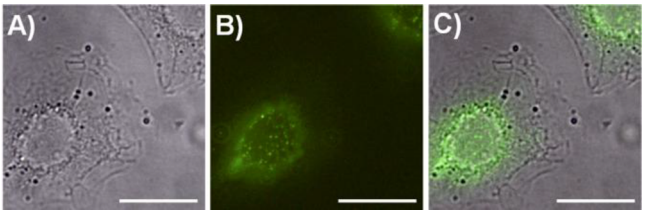

Figure 6. (A) Bright field image of HeLa cells incubated with **2d**. (B) Fluorescence image. (C) Merge of images A and B. The scale bar represents 20 μm.

assay[22] at the same concentration of **2d** as in the marking experiment. These measurements were performed after 24 h incubation of cells with compound **2d** (10^{-3} M solution with less than 1% in DMSO). We found that the cytotoxicity of compound **2d** is 1.3% (Supporting Information). This experiment is the first indication that compound **2d** is highly suitable for further experiments *in vivo*.

■ CONCLUSIONS

In summary, a new modular photoactive boron system based on ONO- and NNN-tridentate ligands has been prepared via a convenient synthetic route. The system exhibits strong blue or green fluorescence, whose color is tuned by facile structural modifications. An axial substituent on the boron atom is useful for the introduction of functional groups. The thermal and chemical stability as well as the acceptable fluorescence quantum yields of 15−40% in solution and in the solid state enable its biochemical use. The versatile application was shown exemplarily for compound **2d** featuring a long alkyl chain at the axial position. This compound is able to form vesicles by itself and can also be used as a marker for nuclear membranes. The low cytotoxicity and the ability to bind to phospholipids are promising results toward the use for further experiments *in vivo*. At present we are investigating the pH dependence of the fluorescence as well as of the vesicle formation. Preliminary results indicate that absorption and emission of compound **2d** show a reversible pH dependence upon treatment with acids and bases due to the presence of the basic iminic nitrogen atoms, which act as proton acceptors. This pH dependence may influence the stability of the vesicles and the preference of **2d** to bind at the nuclear membranes of the HeLa- cells, a prospect we are actively pursuing in current research.

■ EXPERIMENTAL SECTION

General Procedures. Melting points are uncorrected. Nuclear magnetic resonance spectroscopy (^{1}H, ^{13}C, ^{11}B, ^{19}F) were performed on superconductive spectrometers: 300 MHz (^{1}H: 300.1 MHz, ^{13}C: 75.5 MHz, ^{19}F: 282.4 MHz, ^{11}B: 96.3 MHz), 400 MHz (^{1}H: 400.1 MHz, ^{13}C: 100.6 MHz), 500 MHz (^{1}H: 499.9 MHz, ^{13}C: 125.7 MHz, ^{19}F: 470.3 MHz, ^{11}B: 160.4 MHz), and 600 MHz (^{1}H: 599.8 MHz, ^{13}C: 150.8 MHz, ^{19}F: 564.4 MHz, ^{11}B: 192.4 MHz). ^{1}H NMR and ^{13}C NMR chemical shifts δ are given relative to TMS and referenced to the solvent signal. ^{19}F NMR chemical shifts δ are given relative to $CFCl_3$ (external reference). ^{11}B NMR chemical shifts δ are given relative to $BF_3{\cdot}Et_2O$ (external reference). All signals in the ^{1}H NMR and ^{13}C spectra were assigned on the basis of relative intensities, coupling constants, and GCOSY, GHSQC, GHMBC, 1D-COSY, and 1D-NOE experiments. Mass spectra were recorded on a micrOTOF using electron spray ionization. UV−vis absorption spectra were recorded with a resolution of 0.2−0.5 nm. If not stated otherwise, dilute solutions with concentrations of about 10^{-5} M in a 1 cm square quarts cell in degassed dichloromethane were used. Fluorescence lifetimes were measured with a picosecond fluorescence measurement system

dx.doi.org/10.1021/jo4003745 | J. Org. Chem. 2013, 78, 4410−4418

equipped with a picosecond light pulser (excitation wavelength 377 nm with a repetition rate of 10 Hz). Absolute fluorescence quantum yields were determined with a calibrated integrating sphere system. Samples for cryogenic-transmission electron microscopy (cryo-TEM) were prepared by deposition of a few milliliters of vesicle solution of **2d** on holey carbon-coated grids. After blotting the excess liquid, the grids were vitrified in liquid ethane and transferred to a cryo-electron microscope equipped with a cryo-stage, operating at 120 kV. Micrographs were recorded under low-dose conditions with a slow-scan CCD camera. Supplementary crystallographic data for **1a**, **1c**, **2b**, and **2c** (CCDC 895319−895322) can be obtained free of charge via www.ccdc.cam.ac.uk/conts/retrieving.html (or from the Cambridge Crystallographic Data Centre, 12 Union Road, Cambridge, U.K., CB21EZ; fax (+44) 1223-336-03; or deposit@ccdc.cam.ac.uk).

***N,N′*-(Pyridine-2,6-diyl)dibenzamide (3a).** This compound was prepared by modification of a literature procedure.[23a] A suspension of 2,6-diaminopyridine (7.4 g, 67.8 mmol, 1.0 equiv) in dry THF (200 mL) and triethylamine (13.8 g, 136 mmol, 2.0 equiv) was cooled to 0 °C, and benzoyl chloride (19.1 g, 136 mmol, 2.0 equiv) was added dropwise. After evaporation of the solvent the residue was dissolved in dichloromethane and washed with water (3 × 100 mL). The organic layer was dried over $MgSO_4$, and the solvent was evaporated *in vacuo*. Crystallization from ethanol gave *N,N′*-(pyridine-2,6-diyl)dibenzamide as colorless crystals in 74% (15.9 g) yield. The spectroscopic data are consistent with previously published data.[23a]

***N,N′*-(Pyridine-2,6-diyl)bis(4-methylbenzamide) (3b).** This compound was prepared by modification of a literature procedure.[23b] A suspension of 2,6-diaminopyridine (5.5 g, 50.4 mmol, 1.0 equiv) in dry THF (200 mL) and triethylamine (10.1 g, 100 mmol, 2.0 equiv) was cooled to 0 °C, and *p*-toluoyl chloride (15.5 g, 100 mmol, 2.0 equiv) was added dropwise. After evaporation of the solvent the residue was dissolved in dichloromethane and washed with water (3 × 100 mL). The organic layer was dried over $MgSO_4$, and the solvent was evaporated *in vacuo*. Crystallization from ethanol gave *N,N′*-(pyridine-2,6-diyl)bis(4-methylbenzamide) as light brown crystals in 74% (12.9 g) yield. The spectroscopic data are consistent with previously published data.[23b]

***N,N′*-(Pyridine-2,6-diyl)bis(4-methoxybenzamide) (3c).** This compound was prepared by modification of a literature procedure.[23b] A suspension of 2,6-diaminopyridine (3.6 g, 32.7 mmol, 1.0 equiv) in dry THF (100 mL) and triethylamine (6.6 g, 65.4 mmol, 2.0 equiv) was cooled to −10 °C, and a solution of 4-methoxybenzoyl chloride (11.2 g, 65.4 mmol, 2.0 equiv) in THF (50 mL) was added dropwise to the reaction mixture and stirred overnight. The precipitate was filtered off, and the filtrate was concentrated *in vacuo*. The residue was recrystallized from a THF/pentane mixture to give *N,N′*-(pyridine-2,6-diyl)bis(4-methoxybenzamide) as light brown crystals in 58% (7.2 g) yield. The spectroscopic data are consistent with previously published data.[23b]

***N,N′*-(Pyridine-2,6-diyl)dibenzenecarboximidamide (4a).** This compound was prepared by modification of a literature procedure.[24] 2,6-Diaminopyridine (5.5 g, 50 mmol, 1.0 equiv), aluminum chloride (13.4 g, 100 mmol, 2.0 equiv), and benzonitrile (10.3 mL, 100 mmol, 2.0 equiv) were mixed together at −15 °C. The mixture was stirred at room temperature for 15 min and was then heated slowly to 180 °C. After 1 h at this temperature the reaction mixture was allowed to cool to room temperature and was dissolved in 0.4 L of diluted HCl (400 mL H_2O + 25 mL HCl conc) while being sonicated. Afterward charcoal was added, and the suspension was stirred for 1 h before it was filtered off. The filtrate was then poured slowly into 10 M NaOH (150 mL). The precipitate was filtered off and washed with H_2O till neutral pH was reached. The residue was recrystallized from acetonitrile and gave a light brown solid in 57% (8.9 g) yield. The spectroscopic data are consistent with previously published data.[24]

***N,N′*-(Pyridine-2,6-diyl)bis(4-methylbenzenecarboximidamide) (4b).** This compound was prepared by modification of a literature procedure.[24] 2,6-Diaminopyridine (11.0 g, 100 mmol, 1.0 equiv), aluminum chloride (26.7 g, 200 mmol, 2.0 equiv), and *p*-methylbenzonitrile (23.4 g, 200 mmol, 2.0 equiv) were mixed together at −15 °C. The mixture was stirred at room temperature for 15 min and was then heated slowly to 180 °C. After 1 h at this temperature the reaction mixture was allowed to cool to room temperature and was dissolved in 0.4 L of diluted HCl (400 mL H_2O + 25 mL HCl conc) while being sonicated. Afterward charcoal was added, and the suspension was stirred for 1 h before it was filtered off. The filtrate was then poured slowly into 10 M NaOH (150 mL). The precipitate was filtered off and washed with H_2O till neutral pH was reached. The residue was recrystallized from a THF/pentane mixture and gave a light yellow solid in 52% (17.8 g) yield. ^{1}H NMR (600 MHz; CD_2Cl_2): δ 7.84 (d, J_{HH} = 6.4 Hz, 4H, -N=C(-)-Ar*H*), 7.67 (t, J_{HH} = 7.7 Hz, 1H, C_5NH_{para}), 7.27 (d, J_{HH} = 7.9 Hz, 4H, C_5NH_{meta}), 6.85 (d, J_{HH} = 7.2 Hz, 2H, Ar*H*), 2.41 (s, 6H, CH_3) ppm. ^{13}C NMR (150 MHz; CD_2Cl_2): δ 160.8 (C_q), 157.0 (C_q), 141.6 (C_q) 139.9 (C_{Ar}), 134.6 (C_q), 129.7, 127.3 (C_{Ar}), 115.5 (C_{Ar}), 21.7 (CH_3) ppm. HRMS (ESI): calcd for $C_{21}H_{21}N_5H$ ([M + H]$^+$) 344.1870, observed 344.1874.

***N,N′*-(Pyridine-2,6-diyl)dicyclohexanecarboximidamide (4c).** This compound was prepared by modification of a literature procedure.[24] 2,6-Diaminopyridine (5.5 g, 50 mmol, 1.0 equiv), aluminum chloride (13.4 g, 100 mmol, 2.0 equiv), and cyclohexanecarbonitrile (11.9 mL, 100 mmol, 2.0 equiv) were mixed together at −10 °C. The mixture was stirred at room temperature for 15 min and was then heated to 180 °C. After 1 h at this temperature the reaction mixture was allowed to cool to room temperature and was dissolved in 0.4 L of diluted HCl (400 mL H_2O + 25 mL HCl conc) while being sonicated. Afterward charcoal was added, and the suspension was stirred for 1 h before it was poured into 10 M NaOH (150 mL) and extracted with dichloromethane/H_2O (4 × 500 mL). The organic layer was dried over $MgSO_4$, and the residue was recrystallized from acetonitrile to give *N,N′*-(pyridine-2,6-diyl)-dicyclohexanecarboximidamide as a white solid in 51% (8.4 g) yield. ^{1}H NMR (600 MHz; CD_2Cl_2): δ 7.53 (t, J_{HH} = 7.8 Hz, 1H, C_5NH_{para}), 6.56 (d, J_{HH} = 6.2 Hz, 2H, C_5NH_{meta}), 2.20−2.11 (m, 2H, CyC*H*), 1.99−1.90 (m, 4H, CyCH_2), 1.87−1.78 (m, 4H, CyCH_2), 1.75−1.64 (m, 2H, CyCH_2), 1.53−1.40 (m, 4H, CyCH_2), 1.39−1.29 (m, 4H, CyCH_2), 1.29−1.19 (m, 2H, CyCH_2) ppm. ^{13}C NMR (150 MHz; CD_2Cl_2): δ 165.1 (C_q), 161.0 (C_q), 139.5 (C_{Ar}), 113.8 (C_{Ar}), 46.9 (CyCH), 31.4, 26.5, 26.4 (CyCH$_2$) ppm. HRMS (ESI): calcd for $C_{19}H_{29}N_5H$ ([M + H]$^+$) 328.2496, observed 328.2501.

4-(Octadecyloxy)phenyl Boronic Acid. This compound was prepared by modification of a literature procedure.[25] A suspension of 4-bromphenol (17.3 g, 100 mmol, 1.0 equiv), 1-bromooctadecane (36.7 g, 110 mmol, 1.1 equiv), and K_2CO_3 (28.0 g, 200 mmol, 2.0 equiv) in 2-butanone (150 mL) was heated under reflux and vigorous stirring for 24 h. Then the reaction mixture was filtered, and the filtrate was evaporated *in vacuo*. The residue was recrystallized from ethanol and was used for the next step. A solution of 1-bromo-4-octadecyloxyphenyl (4.3 g, 10 mmol, 1.0 equiv) in THF (20 mL) was cooled to −70 °C, and *n*-butyllithium (9.4 mL, 1.6 M in hexane, 15 mmol, 1.5 equiv) was added dropwise. After the reaction mixture was stirred for 0.5 h, triisopropyl borate (2.8 g, 15 mmol, 1.5 equiv) was added at −70 °C. The reaction mixture was warmed to −20 °C and HCl (2 N, 100 mL) was added. After reaching room temperature, the organic layer was separated, and the aqueous layer was extracted with diethylether (3 × 50 mL). The collected organic layers were washed with saturated NaCl solution (3 × 50 mL) and dried over $MgSO_4$. The solvent was removed *in vacuo* and gave the target compound as a white powder in 90% (3.5 g) yield. The spectroscopic data are consistent with previously published data.[25]

Synthesis of Boron Compounds 1a−1c Based on ONO-Tridentate Ligands. Synthesis of 1a. A suspension of *N,N′*-(pyridine-2,6-diyl)dibenzamide (1.0 g, 3.28 mmol, 1.0 equiv) in toluene (25 mL) was cooled to 0 °C, and $BF_3{\cdot}OEt_2$ (1.2 mL, 9.84 mmol, 3.0 equiv) was added dropwise. After removal of the ice bath, the reaction mixture was refluxed for 5 h. The reaction mixture was allowed to cool, and a $NaHCO_3$/DCM mixture (25/50 mL) was added to the solution. The organic layer was collected and washed with $NaHCO_3$ (3 × 50 mL), and the aqueous layer was extracted with DCM (3 × 50 mL). After drying of the collected organic layers over

dx.doi.org/10.1021/jo4003745 | J. Org. Chem. 2013, 78, 4410−4418

Na_2SO_4, the solvent was evaporated *in vacuo*, and the residue was purified via recrystallization from ethyl acetate/heptane to give bright yellow crystals in 90% (1.0 g) yield: mp 214 °C. ^{1}H NMR (500 MHz; CD_2Cl_2): δ 8.41−8.32 (m, 4H, -N=C(-)-Ar*H*), 8.06 (t, J_{HH} = 8.1 Hz, 1H, C_5NH_{para}), 7.67−7.58 (m, 2H, -N=C(-)-ArH_{para}), 7.57−7.47 (m, 4H, -N=C(-)-Ar*H*), 7.23 (d, J_{HH} = 8.1 Hz, 2H, C_5NH_{ortho}) ppm. ^{13}C NMR (125 MHz; CD_2Cl_2): δ 165.5 (*C*=N), 150.4 ($C_{q,Pyridin}$), 145.7 ($C_{Ar,Pyridin,para}$), 133.5 (-N=C(-)-$C_{Ar,para}$), 132.9 (-N=C(-)-C_q), 129.7, 128.8 (-N=C(-)-C_{Ar}), 117.5 ($C_{Ar,Pyridin,meta}$) ppm. ^{11}B NMR (160 MHz; CD_2Cl_2): δ 1.3 (d, $J_{BF} \approx$ 33 Hz, B_{quart}-F) ppm. ^{19}F NMR (470 MHz; CD_2Cl_2): δ −123.36 (1:1:1:1 q, $J_{FB} \approx$ 33 Hz, B_{quart}-*F*) ppm. HRMS (ESI): calcd for $C_{19}H_{13}BFN_3O_2Na$ ([M + Na]$^+$) 368.0980, observed 368.0978.

Synthesis of 1b. A suspension of *N*,*N*′(pyridine-2,6-diyl)bis(4-methylbenzamide) (13.8 g, 39.95 mmol, 1.0 equiv) in toluene (200 mL) was cooled to 0 °C, and BF_3·OEt_2 (15 mL, 119.0 mmol, 3.0 equiv) was added dropwise. After removal of the ice bath, the reaction mixture was refluxed for 5 h. The reaction mixture was allowed to cool, and a $NaHCO_3$/DCM mixture (100/200 mL) was added to the solution. The organic layer was collected and washed with $NaHCO_3$ (3 × 100 mL), and the aqueous layer was extracted with DCM (3 × 100 mL). After drying of the collected organic layers over Na_2SO_4, the solvent was evaporated *in vacuo*, and the residue was purified via alumina oxide B with 5% ethyl acetate and 95% toluene (R_f = 0.83) to give a bright yellow solid in 85% (12.7 g) yield: mp 230 °C. ^{1}H NMR (500 MHz; CD_2Cl_2): δ 8.26−8.22 (m, 4H, -N=C(-)-ArH_{ortho}), 8.02 (t, J_{HH} = 8.1 Hz, 1H, C_5NH_{para}), 7.35−7.31 (m, 4H, -N=C(-)-ArH_{meta}), 7.37 (d, J_{HH} = 8.1 Hz, 2H, C_5NH_{ortho}), 2.45 (s, 6H, CH_3) ppm. ^{13}C NMR (125 MHz; CD_2Cl_2): δ 165.8 (*C*=N), 150.7 ($C_{q,Pyridin}$), 145.7 ($C_{Ar,Pyridin,para}$), 144.8, 130.4 (-N=C(-)-C_q), 129.9, 129.8 (-N=C(-)-C_{Ar}), 117.3 ($C_{Ar,Pyridin,meta}$), 22.1 (CH_3) ppm. ^{11}B NMR (160 MHz; CD_2Cl_2): δ 1.3 (d, $J_{FB} \approx$ 33 Hz, B_{quart}-F) ppm. ^{19}F NMR (470 MHz; CD_2Cl_2): δ −123.78 (1:1:1:1 q, $J_{FB} \approx$ 33 Hz, B_{quart}-*F*) ppm. HRMS (ESI): calcd for $C_{21}H_{17}BFN_3O_2Na$ ([M + Na]$^+$) 396.1294, observed 396.1287.

Synthesis of 1c. A mixture of *N*,*N*′-(pyridine-2,6-diyl)bis(4-methoxybenzamide) (383 mg, 1.01 mmol, 1.0 equiv) and triethylamine (1.42 mL, 10.15 mmol, 10 equiv) in toluene (25 mL) was cooled to 0 °C, and BF_3·OEt_2 (1.9 mL, 10.15 mmol, 10 equiv) was added dropwise. After removal of the ice bath, the reaction mixture was refluxed for 5 h. The reaction mixture was allowed to cool, and a H_2O/DCM mixture (50/100 mL) was added to the solution. The organic layer was collected and washed with H_2O (3 × 50 mL), and the aqueous layer was extracted with DCM (3 × 50 mL). After drying of the collected organic layers over Na_2SO_4, the solvent was evaporated *in vacuo*, and the residue was recrystallized from a ethyl acetate/heptane mixture to give bright yellow crystals in 72% (295 mg) yield. ^{1}H NMR (600 MHz; CD_2Cl_2): δ 8.32−8.28 (m, 4H, -N=C(-)-ArH_{ortho}), 7.99 (t, J_{HH} = 8.1 Hz, 1H, C_5NH_{para}), 7.12 (d, J_{HH} = 8.1 Hz, 2H, C_5NH_{ortho}), 7.02−6.9 (m, 4H, -N=C(-)-ArH_{meta}), 3.90 (s, 6H, CH_3) ppm. ^{13}C NMR (150 MHz; CD_2Cl_2): δ 165.2 (*C*=N), 164.3 (C_q-OMe), 150.6 ($C_{q,Pyridin}$), 145.4 ($C_{Ar,Pyridin,para}$), 131.8 (-N=C(-)-C_{Ar}), 125.2 (-N=C(-)-C_q), 116.6 ($C_{Ar,Pyridin,meta}$), 114.2 (-N=C(-)-C_{Ar}), 55.9 (O-CH_3) ppm. ^{11}B NMR (192 MHz; CD_2Cl_2): δ 1.2 (d, $J_{FB} \approx$ 33 Hz, B_{quart}-F) ppm. ^{19}F NMR (564 MHz; CD_2Cl_2): δ −124.67 (1:1:1:1 q, $J_{FB} \approx$ 33 Hz, B_{quart}-*F*) ppm. HRMS (ESI): calcd for $C_{21}H_{17}BFN_3O_4Na$ ([M + Na]$^+$) 428.1192, observed 428.1199.

Synthesis of Boron Compounds 2a−2d Based on NNN-Tridentate Ligands. General Procedures. The boron complexes based on NNN-tridentate ligands can be obtained by either reacting one equivalent of the respective ligand **4a**-**4c** with an equimolar amount of boronic acid or by reacting one equivalent of the respective ligand **4a**-**4c** with an equimolar amount of triphenylborane. The reaction mixture is refluxed for approximately four hours in toluene in both cases. The purification method used for each compound is given in in the respective experimental section.

Synthesis of 2a. A stirred suspension of phenyl boronic acid (124 mg, 1.02 mmol, 1.0 equiv) and *N*,*N*′-(pyridine-2,6-diyl)-dibenzenecarboximidamide (322 mg, 1.02 mmol, 1.0 equiv) was refluxed in toluene for 5 h. After cooling to room temperature, the solvent was removed *in vacuo*. Purification of the residue on alumina oxide B with 90% toluene and 10% ethyl acetate (R_f = 0.23) afforded compound **2a** in 47% (192 mg) yield as a yellow solid: mp 233 °C. ^{1}H NMR (500 MHz; CD_2Cl_2): δ 8.08−7.94 (m, 4H, -N=C(-)-ArH_{ortho}), 7.61 (t, J_{HH} = 8.0 Hz, 1H, C_5NH_{para}), 7.57−7.53 (m, 2H, -N=C(-)-ArH_{para}), 7.51−7.45 (m, 4H, -N=C(-)-ArH_{meta}), 7.37 (dd, J_{HH} = 7.9, 1.4 Hz, 2H, -B-ArH_{ortho}), 7.25−7.09 (m, 3H, -B-Ar$H_{meta,para}$), 6.76 (d, J_{HH} = 8.0 Hz, 2H, C_5NH_{ortho}), 6.30 (s, 2H, N*H*) ppm. ^{13}C NMR (125 MHz; CD_2Cl_2): δ 162.4 (*C*=N), 153.4 ($C_{q,Pyridin}$), 142.7 ($C_{Ar,Pyridin,para}$), 136.1 (-N=C(-)-C_q), 132.0 (-N=C(-)-$C_{Ar,para}$), 130.4 (-B-$C_{Ar,ortho}$), 129.2 (-N=C(-)-$C_{Ar,meta}$), 128.3, 127.9 (-B-$C_{Ar,meta,para}$), 127.5 (-N=C(-)-$C_{Ar,ortho}$), 114.3 ($C_{Ar,Pyridin,meta}$) ppm. (The B-C_q signal was not observed due to the quadrupolar relaxation of the boron atom). ^{11}B NMR (160 MHz; CD_2Cl_2): δ −1.2 (s, B_{quart}) ppm. HRMS (ESI): calcd for $C_{25}H_{20}BN_5H$ ([M + H]$^+$) 402.1889, observed 402.1888.

Synthesis of 2b. A stirred suspension of phenyl boronic acid (135.3 mg, 1.11 mmol, 1.0 equiv) and *N*,*N*′-(pyridine-2,6-diyl)bis(4-methylbenzenecarboximidamide) (381.1 mg, 1.11 mmol, 1.0 equiv) was refluxed in toluene for 5 h. After cooling to room temperature, the solvent was removed *in vacuo*. Purification of the residue on alumina oxide B with 90% toluene and 10% ethyl acetate (R_f = 0.30) afforded compound **2b** in 67% (319 mg) yield as a yellow solid: mp 240 °C. ^{1}H NMR (500 MHz; CD_2Cl_2): δ 7.92−7.87 (m, 4H, -N=C(-)-ArH_{ortho}), 7.57 (t, J_{HH} = 8.0 Hz, 1H, C_5NH_{para}), 7.35 (dd, J_{HH} = 7.9, 1.4 Hz, 2H, -B-ArH_{ortho}), 7.31−7.27 (m, 4H, -N=C(-)-ArH_{meta}), 7.20−2.11 (m, 3H, −B-Ar$H_{meta,para}$), 6.70 (d, J_{HH} = 8.0 Hz, 2H, C_5NH_{meta}), 6.46 (s, 2H, N*H*), 2.42 (s, 6H, −CH_3) ppm. ^{13}C NMR (125 MHz; CD_2Cl_2): δ 162.1 (*C*=N), 153.5 ($C_{q,Pyridin}$), 142.6 ($C_{Ar,Pyridin}$), 142.5 (C_q), 133.3 (C_q), 130.4, 129.8, 128.2, 127.7, 127.5 (C_{Ar}), 114.3 ($C_{Ar,Pyridin}$), 21.8 (CH_3) ppm. (The B-C_q signal was not observed due to the quadrupolar relaxation of the boron atom). ^{11}B NMR (160 MHz; CD_2Cl_2): δ −1.3 (s, B_{quart}) ppm. HRMS (ESI): calcd for $C_{27}H_{24}BN_5H$ ([M + H]$^+$) 430.2202, observed 430.2208.

Synthesis of 2c. A stirred suspension of phenyl boronic acid (179 mg, 1.47 mmol, 1.0 equiv) and *N*,*N*′-(pyridine-2,6-diyl)-dicyclohexanecarboximidamide (481 mg, 1.47 mmol, 1.0 equiv) was refluxed in toluene for 5 h. After cooling to room temperature, the solvent was removed *in vacuo*. Purification of the residue on alumina oxide B with 80% hexane and 20% ethyl acetate (R_f = 0.72) afforded compound **2c** in 43% (261 mg) yield as a light yellow solid: mp 180 °C. ^{1}H NMR (600 MHz; C_6D_6): δ 7.72−7.45 (m, 2H, ArH_{ortho}), 7.32 (t, J_{HH} = 7.6 Hz, 2H, ArH_{meta}), 7.20−7.16 (m, 1H, ArH_{para}), 6.83 (t, J_{HH} = 8.0 Hz, 1H, C_5NH_{para}), 6.58 (d, J_{HH} = 8.0 Hz, 2H, C_5NH_{ortho}), 5.15 (s, 2H, N*H*), 2.11 (tt, J_{HH} = 11.9, 3.4 Hz, 2H, CyC*H*), 1.95 (d, J_{HH} = 11.9 Hz, 4H, CyCH_2), 1.74−1.61 (m, 4H, CyCH_2), 1.61−1.48 (m, 6H, CyCH_2), 1.22−0.98 (m, 6H, CyCH_2) ppm. ^{13}C NMR (150 MHz; C_6D_6): δ 172.0 (*C*=N), 153.6 ($C_{q,Pyridin}$), 142.5 ($C_{Ar,Pyridin}$), 130.2, 128.1, 127.6 (C_{Ar}), 112.9 ($C_{Ar,Pyridin}$), 47.1 (CyCH), 31.4, 31.1, 26.6, 26.5, 26.5 (CyCH_2) ppm. (The B-C_q signal was not observed due to the quadrupolar relaxation of the boron atom). ^{11}B NMR (192 MHz; C_6D_6): δ −2.7 (s, B_{quart}) ppm. HRMS (ESI): calcd for $C_{25}H_{32}BN_5H$ ([M + H]$^+$ 414.2828, observed 414.2827.

Synthesis of 2d. A stirred suspension of 4-(octadecyloxy)phenyl boronic acid (423.0 mg, 1.08 mmol, 1.0 equiv) and *N*,*N*′-(pyridine-2,6-diyl)dibenzenecarboximidamide (342.0 mg, 1.08 mmol, 1.0 equiv) was refluxed in toluene for 4 h. After cooling to room temperature, the solvent was removed *in vacuo*. Purification of the residue on alumina oxide B with 90% cyclohexane and 10% ethyl acetate (R_f = 0.12) afforded compound **2d** in 65% (470 mg) yield as a yellow solid: mp 160 °C. ^{1}H NMR (500 MHz; CD_2Cl_2): δ 8.03−7.96 (m, 4H, -N=C(-)-Ar*H*), 7.59 (t, J_{HH} = 8.0 Hz, 1H, C_5NH_{para}), 7.57−7.52 (m, 2H, -N=C(-)-Ar*H*), 7.52−7.46 (m, 4H, -N=C(-)-Ar*H*), 7.30−7.25 (m, 2H, -B-ArH_{ortho}), 6.74 (d, J_{HH} = 8.0 Hz, 2H, C_5NH_{ortho}), 6.73−6.69 (m, 2H, -B-ArH_{meta}), 6.28 (s, 2H, N*H*), 3.85 (t, J_{HH} = 6.6 Hz, 2H, -O$CH_2CH_2CH_2(CH_2)_{14}CH_3$), 1.74−1.63 (m, 2H, -O$CH_2CH_2CH_2(CH_2)_{14}CH_3$), 1.43−1.34 (m, 2H, -O$CH_2CH_2CH_2(CH_2)_{14}CH_3$), 1.34−1.22 (m, 28H, -O$CH_2CH_2CH_2(CH_2)_{14}CH_3$), 0.95−0.78 (m, 3H, -O$CH_2CH_2CH_2(CH_2)_{14}CH_3$) ppm. ^{13}C NMR (125 MHz; CD_2Cl_2):

dx.doi.org/10.1021/jo4003745 | *J. Org. Chem.* 2013, 78, 4410−4418

δ 162.4 (C=N), 159.4 (C_q-$OC_{18}H_{37}$), 153.3 ($C_{q,Pyridin}$), 142.5 ($C_{Ar,Pyridin,para}$), 136.2 (-N=C(-)-C_q), 131.9 (-N=C(-)-C_{Ar}), 131.6 (-B-C_{Ar}), 129.2, 127.5 (-N=C(-)-C_{Ar}), 114.3 ($C_{Ar,Pyridin,meta}$), 114.4 (-B-C_{Ar}), 68.3 (-$OCH_2CH_2CH_2(CH_2)_{14}CH_3$), 32.5, 30.3, 30.0, 29.9 (-$OCH_2CH_2CH_2(CH_2)_{14}CH_3$), 26.6 (-$OCH_2CH_2CH_2(CH_2)_{14}CH_3$), 23.3 (-$OCH_2CH_2CH_2(CH_2)_{14}CH_3$), 14.5 (-$OCH_2CH_2CH_2(CH_2)_{14}CH_3$) ppm. (The B-$C_q$ signal was not observed due to the quadrupolar relaxation of the boron atom). ^{11}B NMR (160 MHz; CD_2Cl_2): δ −1.3 (s, B_{quart}) ppm. HRMS (ESI): calcd for $C_{43}H_{56}BN_5OH$ ($[M + H]^+$) 670.4658, observed 670.4660.

■ ASSOCIATED CONTENT

Supporting Information

Experimental and quantum chemical details are available free of charge via the Internet at http://pubs.acs.org.

■ AUTHOR INFORMATION

Corresponding Author

*E-mail: wurthwe@uni-muenster.de; yamaguchi@chem.nagoya-u.ac.jp.

Notes

The authors declare no competing financial interest.

■ ACKNOWLEDGMENTS

Financial support from the Deutsche Forschungsgemeinschaft (IRTG 1143 Münster-Nagoya and SFB 858) is gratefully acknowledged.

■ DEDICATION

Dedicated to Prof. Werner Uhl on the occasion of his 60th birthday.

■ REFERENCES

(1) (a) Entwistle, C. D.; Marder, T. B. *Angew. Chem., Int. Ed.* **2002**, *41*, 2927−2931. (b) Entwistle, C. D.; Marder, T. B. *Chem. Mater.* **2004**, *16*, 4547−4585. (c) Jäkle, F. *Coord. Chem. Rev.* **2006**, *250*, 1107−1121. (d) Yamaguchi, S.; Wakamiya, A. *Pure Appl. Chem.* **2006**, *78*, 1413−1424. (e) Loudet, A.; Burgess, K. *Chem. Rev.* **2007**, *107*, 4891−4932. (f) Bosdet, M. J. D.; Piers, W. E. *Can. J. Chem.* **2009**, *87*, 8−29. (g) Ulrich, G.; Ziessel, R.; Harriman, A. *Angew. Chem., Int. Ed.* **2008**, *47*, 1184−1201. (h) Wade, C. R.; Broomsgrove, A. E. J.; Aldrige, S.; Gabbaï, F. P. *Chem. Rev.* **2010**, *110*, 3958−3984. (i) Jäkle, F. *Chem. Rev.* **2010**, *110*, 3985−4022. (j) Neue, B.; Fröhlich, R.; Wibbeling, B.; Fukazawa, A.; Wakamiya, A.; Yamaguchi, S.; Würthwein, E.-U. *J. Org. Chem.* **2012**, *77*, 2176−2184. (k) Tanaka, K.; Chujo, Y. *Macromol. Rapid Commun.* **2012**, *33*, 1235−1255.

(2) (a) Gonçalves, M. S. T. *Chem. Rev.* **2009**, *109*, 190−212. (b) Hayek, A.; Bolze, F.; Bourgogne, C.; Baldeck, P. L.; Didier, P.; Arntz, Y.; Mély, Y.; Nicoud, J.-F. *Inorg. Chem.* **2009**, *48*, 9112−9119. (c) Thorp-Greemwood, F. L. *Organometallics* **2012**, *31*, 5686−5692.

(3) (a) Morse, G. E.; Bender, T. P. *ACS Appl. Mater. Interfaces* **2012**, *4*, 5055−5068. (b) Hudson, Z. M.; Wang, S. *Dalton Trans.* **2011**, *40*, 7805−7816.

(4) (a) Rousseau, T.; Cravino, A.; Bura, T.; Ulrich, G.; Ziessel, R.; Roncali, J. *J. Mater. Chem.* **2009**, *19*, 2298−2300. (b) Kumaresan, D.; Thummel, R. P.; Bura, T.; Ulrich, G.; Ziessel, R. *Chem.—Eur. J.* **2009**, *15*, 6335−6339. (c) Chen, P.; Lalancette, R. A.; Jäkle, F. *Angew. Chem., Int. Ed.* **2012**, *51*, 1−6. (d) Rao, Y.-L.; Amarne, H.; Zhao, S.-B.; McCormick, T. M.; Martic, S.; Sun, Y.; Wang, R.-Y.; Wang, S. *J. Am. Chem. Soc.* **2008**, *130*, 12898−12900. (e) Rao, Y.-L.; Wang, S. *Inorg. Chem.* **2011**, *50*, 12263−12274.

(5) (a) Rao, Y.-L.; Amarne, H.; Wang, S. *Coord. Chem. Rev.* **2012**, *256*, 759−770. (b) Araneda, J. F.; Piers, W. E.; Heyne, B.; Parvez, M.; McDonald, R. *Angew. Chem.* **2011**, *50*, 12214−12217. (c) Lorbach, A.; Bolte, M.; Li, H.; Lerner, H.-W.; Holthausen, M. C.; Jäkle, F.; Wagner, M. *Angew. Chem., Int. Ed.* **2009**, *48*, 4584−4588. (d) Maeda, H.; Ito, Y.; Haketa, Y.; Eifuku, N.; Lee, E.; Lee, M.; Hashishin, T.; Kaneko, K. *Chem.—Eur. J.* **2009**, *15*, 3706−3719.

(6) (a) Caballero, E.; Fernández-Ariza, J.; Lynch, V. M.; Romero-Nieto, C.; Rodríguez-Morgade, M. S.; Sessler, J. L.; Guldi, D. M.; Torres, T. *Angew. Chem., Int. Ed.* **2012**, *51*, 11337−11342. (b) Claessens, C. G.; González-Rodríguez, D.; Torres, T. *Chem. Rev.* **2002**, *102*, 835−853. (c) Guilleme, J.; González-Rodríguez, D.; Torres, T. *Angew. Chem., Int. Ed.* **2011**, *50*, 3506−3509. (d) Osuka, A.; Tsurumaki, E.; Tanaka, T. *Bull. Chem. Soc. Jpn.* **2011**, *84*, 679−697. (e) Zhang, H.; Huo, C.; Ye, K.; Zhang, P.; Tian, W.; Wang, Y. *Inorg. Chem.* **2006**, *45*, 2788−2794. (f) Mysliborski, R.; Latos-Grażyński, L.; Szterenberg, L.; Lis, T. *Angew. Chem., Int. Ed.* **2006**, *45*, 3670−3674. (g) Gonzáles-Rodríguez, D.; Torres, T.; Guldi, D. M.; Rivera, J.; Herranz, M. A.; Echegoyen, L. *J. Am. Chem. Soc.* **2004**, *126*, 6301−6313.

(7) Häger, I.; Fröhlich, R.; Würthwein, E.-U. *Eur. J. Inorg. Chem.* **2009**, *16*, 2415−2428.

(8) El-Shazly, M. F.; El-Disskowky, A.; Salem, T.; Osman, M. *Inorg. Chim. Acta* **1980**, *40*, 1−6.

(9) (a) Cooper, F. C.; Partridge, M. W. *Org. Synth.* **1963**, *36*, 64. (b) Koutentis, P. A.; Mirallai, S. I. *Tetrahedron* **2010**, *66*, 5134−5139.

(10) Tajbakhsh, A. R.; Dias, F. B.; Zheng, Y.; Wright, P. V. *Mol. Cryst. Liq. Cryst. Sci. Technol., Sect. A* **1998**, *323*, 69−87.

(11) (a) Kitamura, C.; Tanigawa, Y.; Kobayashi, T.; Naito, H.; Kurata, H.; Kawase, T. *Tetrahedron* **2012**, *68*, 1688−1694. (b) Dreuw, A.; Plötner, J.; Lorenz, L.; Wachtveitl, J.; Djanhan, J. E.; Brüning, J.; Metz, T.; Bolte, M.; Schmidt, M. U. *Angew. Chem., Int. Ed.* **2005**, *44*, 7783−7786. (c) Langhals, H.; Potrawa, T.; Nöth, H.; Linti, G. *Angew. Chem., Int. Ed. Engl.* **1989**, *28*, 478−480.

(12) Lee, C.; Yang, W.; Parr, R. G. *Phys. Rev. B* **1988**, *37*, 785−789.

(13) Yanai, T.; Tew, D. P.; Handy, N. C. *Chem. Phys. Lett.* **2004**, *393*, 51−57.

(14) (a) Brooker, L. G. S.; Keyes, G. H.; Sprague, R. H.; VanDyke, R. H.; VanLare, E.; VanZandt, G.; White, F. L. *J. Am. Chem. Soc.* **1951**, *73*, 5326−5332. (b) Brooker, L. G. S.; Keyes, G. H.; Heseltine, D. W. *J. Am. Chem. Soc.* **1951**, *73*, 5350−5356.

(15) Weber, L.; Kuhtz, H.; Böhling, L.; Brockhinke, A.; Chrostowska, A.; Dargelos, A.; Mazière, A.; Stammler, H.-G.; Neumann, B. *Dalton Trans.* **2012**, *41*, 10440−10452.

(16) Kunitake, T. *Angew. Chem., Int. Ed. Engl.* **1992**, *31*, 709−726.

(17) Voskuhl, J.; Ravoo, B. J. *Chem. Soc. Rev.* **2009**, *38*, 495−505.

(18) (a) Dong, R.; Zhu, B.; Zhou, Y.; Yan, D.; Zhu, X. *Angew. Chem., Int. Ed.* **2012**, *51*, 11633−11637. (b) Zhang, X.; Rehm, S.; Safont-Sempere, M. M.; Würthner, F. *Nat. Chem.* **2009**, *1*, 623−629. (c) Ryu, J. H.; Hong, D. J.; Lee, M. *Chem. Commun.* **2008**, 1043−1054.

(19) Cheng, F.; Bonder, E. M.; Jäkle, F. *Macromolecules* **2012**, *45*, 3078−3085.

(20) Nagai, A.; Kokado, K.; Miyake, J.; Chujo, Y. *Macromolecules* **2009**, *42*, 5446−5452.

(21) Cheng, F.; Jäkle, F. *Polym. Chem.* **2011**, *2*, 2122−2132.

(22) *CytoTox 96 Non-Radioactive Cytotoxicity Assay, Technical Bulletin*, Part no. TB163; Promega Corp.: Madison, WI, 2009; pp 1−17.

(23) (a) Yu, L.; Schneider, H.-J. *Eur. J. Org. Chem.* **1999**, *1999*, 1619−1625. (b) Langer, P.; Amiri, S.; Bodtke, A.; Saleh, N. N. R.; Weisz, K.; Görls, H.; Schreiner, P. R. *J. Org. Chem.* **2008**, *73*, 5048−5063.

(24) Leitch, A. A.; Oakley, R. T.; Reed, R. W.; Thompson, L. K. *Inorg. Chem.* **2007**, *46*, 6261−6270.

(25) Tajbakhsh, A. R.; Dias, F. B.; Zheng, Y.; Wright, P. V. *Mol. Cryst. Liq. Cryst. Sci. Technol., Sect. A* **1998**, *323*, 69−87.